magnetochemistry

MDPI

Article

Comparative Magnetic Studies in the Solid State and Solution of Two Isostructural 1D Coordination Polymers Containing Co^{II}/Ni^{II}-Curcuminoid Moieties

Raúl Díaz-Torres [1,2], Melita Menelaou [1], Arántzazu González-Campo [2], Simon J. Teat [3], E. Carolina Sañudo [1,4], Mónica Soler [5,*] and Núria Aliaga-Alcalde [2,6,*]

1 Departament de Química Inorgànica i Orgànica, Secció d' Inorgànica, Universitat de Barcelona, Diagonal 645, 08028 Barcelona, Spain; rauldiaztor@gmail.com (R.D.-T.); mmelenaou@qi.ub.es (M.M.); esanudo@ub.edu (E.C.S.)

2 CSIC-ICMAB (Institut de Ciència dels Materials de Barcelona) Campus de la Universitat Autònoma de Barcelona, 08193 Bellaterra, Spain; agonzalez@icmab.es

3 Advanced Light Source, Lawrence Berkeley National Laboratory, Berkeley, CA 94720, USA; sjteat@lbl.gov

4 Institut de Nanociència i Nanotecnologia, Universitat de Barcelona, Av. Diagonal 645, 08028 Barcelona, Spain

5 Departamento de Ciencia de los Materiales, Facultad de Ciencias Físicas y Matemáticas, Universidad de Chile, Beaucheff 851, Santiago, Chile

6 ICREA (Institució Catalana de Recerca i Estudis Avançats), Pg. Lluís Companys 23, 08010 Barcelona, Spain

* Correspondence: msoler@ing.uchile.cl (M.S.); nuria.aliaga@icrea.cat (N.A.-A.); Tel.: +56-2-297-84240 (M.S.); +34-935-801-853 (N.A.-A.)

Academic Editor: Carlos J. Gómez García
Received: 16 June 2016; Accepted: 19 July 2016; Published: 29 July 2016

Abstract: Two novel 1D coordination chains containing the curcuminoid (CCMoid) ligand 9Accm have been characterized: $[Co^{II}(9Accm)_2(4,4'\text{-bpy})]_n$ (**1**) and $[Ni^{II}(9Accm)_2(4,4'\text{-bpy})]_n$ (**2**). The two compounds were synthesized by solvothermal and microwave (MW) assisted techniques, respectively, and crystals of both systems were directly obtained from the mother solutions. Crystal structures of **1** and **2** prove that both systems are isostructural, with the ligands in a *trans* configuration. The two chains have been magnetically characterized in solution by paramagnetic ^{1}H NMR, where **1** displayed typical features from Co^{II} systems, with spread out signals; meanwhile, **2** showed diamagnetic behaviour. The dissociation of the latest in solution and the stability of the "$[Ni(9Accm)_2]$" unit were proved by further experiments in C_5D_5N. Additional UV-Vis absorption and fluorescence studies in solution were performed using exclusively **1**. In the solid state $\chi_M T$ vs. T and $M/N\mu_B$ vs. H/T data were collected and fitted for **1** and **2**; both systems display Ising plane anisotropy, with significant D values. System **1** presented slow relaxation of the magnetization, displaying frequency dependence in the in-phase/out-phase ac magnetic susceptibility data, when an external dc field of 0.2 T was applied. Finally, **1** was deposited on a HOPG (highly oriented pyrolytic graphite) substrate by spin-coating and analysed by AFM.

Keywords: curcumin derivatives; curcuminoid; building block; 1D coordination chain; SMM; SCM; slow relaxation of magnetization; paramagnetic NMR; fluorescence; AFM; HOPG surface

1. Introduction

Single-molecule magnets (SMMs) [1] and single-chain magnets (SCMs) [2] are promising candidates as components in high-density storage and/or spintronics devices [3–6]. Regarding SMMs, a fast-growing number of mononuclear 3d/4f compounds that display slow relaxation of the magnetization have recently been introduced [7–9]. In this regard, the use of external magnetic fields to cancel an often-present fast zero-field relaxation of the magnetization [10,11], as well as the observation

of frequency dependence in 3D mononuclear species with negative but also positive [12,13] zero-field splitting (*D*) values, have been key factors toward the development of the subject. Indeed, the SMM character of compounds with a positive *D* parameter has shaken up a well-established requirement for the occurrence of this unique behaviour.

From a synthetic point of view, the first outcome, from the arising of mononuclear SMMs, is the release from the restrictions of "serendipitous self-assembly" methods widely employed toward the formation of novel high-nuclearity SMMs. Where in the past the structural complexity of the molecular systems made, at times, difficult their proper magnetic analyses and slowed down the achievement of improved materials, the application of straightforward designs now allows chemical planning of the final species. Even though this aspect is still at a premature stage, it will make possible the anticipation of the results. Indeed, nowadays there are models that predict mononuclear 3d-SMMs in a rationalized way [10], and therefore, using such information with the right organic connectors, we may be able to tune SCM behaviour as well. Nevertheless, the proper progress of this subject requires a deep insight regarding extra factors that can affect the final properties [3–6,13,14].

Additional and innovative aspects are the employment of ligands to implement new or supplementary properties as well as the deposition of SMMs/SCMs, in an organized manner, on substrates toward their future inclusion as components in nanodevices. The creation of suitable functional materials with relevant magnetic properties is also a hot topic in areas such as molecular electronics and spintronics [3–6], where controlling the molecular/chain disposition at the nanoscale is crucial. In this sense, mononuclear coordination compounds provide the opportunity of achieving independent units that eventually can function as building blocks in more elaborate structures.

Regarding the latest idea, here we report our first studies with two isostructural Co^{II}/Ni^{II} chains, systems **1** and **2**, containing a curcuminoid (CCMoid) ligand, described before, called 9Accm [15–20]. Systems **1** and **2** are coordination polymers formed by the periodic repetition of "$[M(9Accm)_2]$" units linked through 4,4'-bpy molecules, well known as structural connectors [21]. In a recent work we gathered detailed information about two mononuclear $[Co^{II}(9Accm)_2X_m]$ compounds (X = py (m = 2), 2,2'-bpy (m = 1)), both SMMs, and have studied the impact of the *trans*/*cis* disposition of the ligands on their magnetic response [22]. Guided by previous results, we now show the study where small mononuclear units of "$[Co^{II}(9Accm)_2(solvent)_2]$" and "$[Ni^{II}(9Accm)_2]$" are used as building blocks providing coordination chains. We are motivated by the synthetic possibilities of (i) using such units as building blocks for more complex systems, (ii) conducting analysis/modifications of the magnetic properties by the use of a ligand (4,4'-bpy) that provides structural features with very weak or no intermolecular interactions, and (iii) conducting comparative studies between **1** and **2** regarding their stability and magnetic behaviours. We present the crystallographic data of both species as well as the specialized characterization of the magnetic properties of both by paramagnetic ^1H NMR in solution and the use of a SQUID (superconducting quantum interference device) magnetometer in the solid state. From the earliest stage, we have extracted relevant information on the dissociation of chain **2** into stable "$[Ni^{II}(9Accm)_2]$" units. Additional studies in the solution of **1** include UV-Vis absorption and fluorescence experiments. Magnetically, **1** displays slow relaxation of the magnetization, suggesting that it behaves as one 1D SMM. Finally, the deposition of **1** on HOPG substrate is described and compared with its mononuclear analogous.

2. Results and Discussions

Coordination polymers **1** and **2** have been achieved by the use of solvothermal [23] and microwave (MW)-assisted [24] methods, both well-applied to attain mononuclear systems [20,22] and higher-dimensional structures [21,23]. MW-assisted techniques have been used previously in the group and have been described in the past as an effective tool toward the achievement of crystals directly from the reaction. On the other hand, solvothermal methods are currently used in the achievement of MOFs. We used such methodologies with the same objective of accomplishing the formation of crystals directly from the mother solutions. Such facts are very useful with CCMoids, where one

of the difficulties is the achievement of microcrystalline powder with an average size for standard diffractometers. As explained elsewhere [22], the still-remarkable flexibility of the conjugated chain of the 9Accm and its limited solubility may add difficulties toward the achievement of the crystals. In this case, system **1** was characterized by a synchrotron source; meanwhile, the crystallographic data of **2** was resolved by conventional single X-ray diffraction. The following sections relate to the precise methodology and description of the structures.

2.1. Experimental Results

All experiments were carried out in aerobic conditions using commercial-grade solvents for the synthesis of the two compounds. Solvents were distilled for the UV-vis, fluorescence and nano-structuration studies. The 9Accm was synthesized according to the procedure described elsewhere [15].

2.1.1. Synthesis of $[Co(9Accm)_2(4,4´\text{-bpy})]_n$ (**1**)

Compound **1** was synthesized by mixing, in 5 mL of DMF, 0.026 g (0.104 mmol) of $[Co(O_2CMe)_2{\cdot}4H_2O]$, 0.100 g (0.210 mmol) of 9Accm and 0.016 g (0.104 mmol) of 4,4'-bpy in a solvothermal vial. The vial was maintained at 143 °C during two days in the oven (no stirring). Afterward, crystals of **1** where collected. Yield 88%. Anal. calcd for $C_{83}H_{57}CoN_2O_5{\cdot}0.3C_3H_7NO{\cdot}1.3\ H_2O$ (1265.65 g·mol^{-1}): C 79.56; H 4.91; N 2.54. Found: C 79.48; H 4.86; 2.52. IR Data (KBr, cm^{-1}): 3394(br), 3046(w), 2922(w), 2853(w), 1630(m), 1603(m), 1548(s), 1506(s), 1440(s), 1405(s), 1348(m), 1217(m), 1158(m), 975(m), 889(m), 842(m), 807(m), 733(vs), 622(m), 538(w), 446(w). MALDI$^-$ (m/z): 1009.3 ($[Co(9Accm)_2]^-$).

2.1.2. Synthesis of $[Ni(9Accm)_2(4,4´\text{-bpy})]_n$ (**2**)

Compound **2** was achieved by modifying the methodology used elsewhere [20]. The same exact quantities described for **1** were mixed in 5 mL of DMF in a microwave (MW) tube. The reaction mixture was under stirring while a power of 250 MW was applied during 2 min (maximum allowed temperature during the 2 min = 140°). Yellow microcrystals were achieved after cooling down to room temperature. Yield 78%. Anal. calcd for $C_{80}H_{54}NiN_2O_4{\cdot}0.9H_2O$ (1182.56 g·mol^{-1}): C 81.17; H 4.76; N 2.36. Found: C 81.18; H 4.61; N 2.40. IR Data (KBr, cm^{-1}): 3426(br), 3043(w), 2964(w), 2920(w), 2843(w), 1677(w), 1625(m), 1548(s), 1504(vs), 1447(vs), 1410(s), 1348(m), 1212(s), 1158(m), 1109(w), 968(m), 879(w), 839(w), 812(w), 726(s), 617(w), 543(w), 449(w). MALDI$^+$ (m/z): 533.0 ($[Ni_2(9Accm)_2]^{2+}$; 1066.2 ($[Ni(9Accm)_2NaCl]$).

2.2. Structural Description

General crystal data information of the two systems, **1** and **2**, are shown in Table S1. X-ray diffraction analysis of the two species shows that they are isostructural. Compounds **1** and **2** crystallize in the monoclinic space $C2/c$, with similar cell parameters, where their asymmetric coordination units are better described as $[M(9Accm)_2(4,4'\text{-bpy})]$ (being M = Co^{II} or Ni^{II}). Selected bond lengths and angles are listed in Table S2. Figure 1 shows the POV-Ray (persistence of vision Raytracer) view of one isolated fragment of **1** (A) together with a general view emphasizing the intermolecular interactions between different chains of **1** (B). Figure S1 shows the same information for polymer **2**. Both compounds have hexacoordinate M^{II} centres that bind two 9Accm molecules in the equatorial plane of the metal ion and two 4,4'-bipyridine molecules in the axial plane. Co–O/Co–N distances (2.030–2.061 Å/2.137–2.147 Å) and Ni–O/Ni–N distances (2.000–2.042 Å/2.081–2.131 Å) are similar to others published in the past [25]. The pyridinic groups function as a bridge between the neighbouring metallic centres forming 1D chains (Figure 1A). The two aromatic groups of the pyridinic moiety are twisted, preventing co-planarity between the rings, with angles of 25.26° for **1** and 25.56° for **2**, respectively. The *trans* disposition of the 4,4'-bpy molecules and their conjugated nature confers strict linearity to the final chains in both systems, with very similar Co–Co/Ni–Ni distances of 11.337 Å and 11.287 Å, respectively. As has been observed in previous *M*-CCMoid systems (*M* = metal centre) containing monocoordinate

pyridine derivatives [22], the 9Accm ligands are disposed in a *trans* conformation providing an ideal D_{4h} geometry. In both systems, **1** and **2**, such organic ligands show two alternating C–C values related to the double/single bonds, typical of CCMoid chains and similar to others [15–20,22]. The conjugated skeletons of the two species present exclusively zig-zag conformations, when in the past similar mononuclear units have displayed both zig-zag and boat shapes [22]. Both sides of each CCMoid end in anthracene groups that are disposed almost in a perpendicular manner to their CCMoid frames, working as a protecting coat among the chains and therefore strongly attenuating intermolecular interactions among the metallic centres (distances above 13 Å) but also providing interesting σ-π interactions within anthracene groups of the neighbouring chains (Figure 1B). No additional π-π stacking or hydrogen bondings were observed in the two structures.

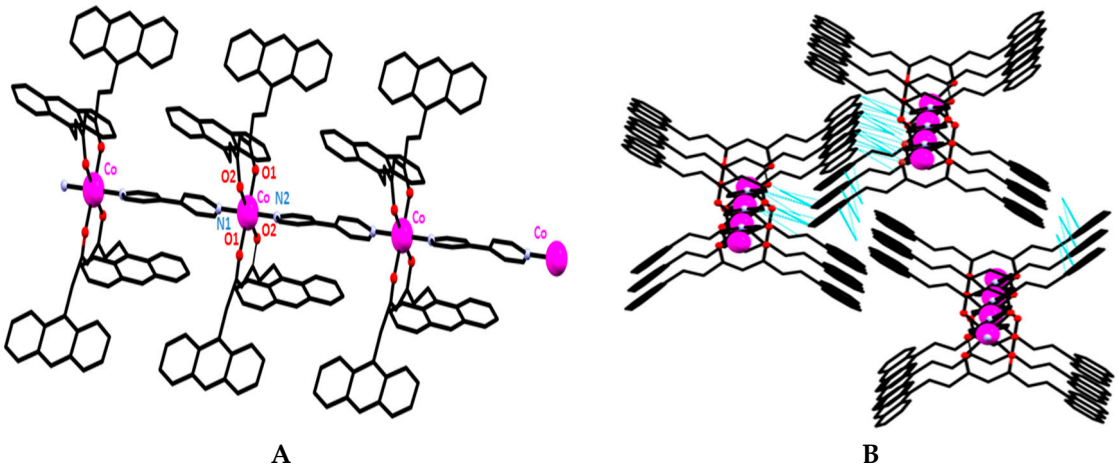

Figure 1. (**A**) POV-Ray (persistence of vision Raytracer) view of one isolated fragment of **1**. Protons are omitted for the sake of simplification. Color legend: Co in pink, O in red, N in blue and C in black. (**B**) POV-Ray view emphasizing intermolecular interactions among different chains of **1** (light blue lines).

2.3. Studies in Solution

2.3.1. Paramagnetic ^{1}H NMR

The ^{1}H NMR spectra of **1** (Figure 2A) and **2** (Figure S2) were measured in $CDCl_3$. In a recent article [22] some of us have shown the relevance of paramagnetic NMR as a fingerprint for the analyses in solution of mononuclear Co^{II} systems containing 9Accm, providing information about stability in solution and the disposition of the CCMoid ligands in the structure. Taking into account these studies, the analysis in solution of compound **1** was performed by comparing it with previous data. System **2** was treated as **1**, as it is known that paramagnetic Ni^{II} systems show slow nuclear relaxation as well, and therefore sharp enough spectral features [26].

The spectrum of compound **1** displays a limited number of signals in the range of −10 to 70 ppm, an aspect that relates to its symmetry in solution (ideally D_{4h}) and additional factors such as rotation of the anthracene groups [22]. It is worth stressing that the spectra did not vary after several hours, indicating that the system was stable at RT under such conditions. Overall, the spectrum can be divided in two regions: one at down field (from 70 to 20 ppm) that contains two unique signals and a second area from 20 ppm to −10 ppm that shows the majority of the signals. In the former, the appearance of a broad signal at 61 ppm related to the –CH– proton of the 9Accm, the closest to the Co^{II} ion, in agreement with the previous mononuclear $[Co(9Accm)_2(py)_2]$ system [22], which shows a similar pattern with a shift at 63 ppm. At the down area spectrum of **1**, the signal appearing at 22 ppm may relate to the *ortho* protons of the 4,4'-bpy molecules. In the high field area, the sharp peaks at −10 and 9 ppm may be also of pyridinic nature and relate to the *para* and *meta* protons,

but in the assignment it is not that simple due to their shape and the existence of several other signals nearby (from 8.7–7.5 ppm) that could be linked to the CCMoid but also to the two aromatic rings from the 4,4'-bpy. Finally, two important pieces of information can be extracted from these experiments: (i) the stability of the system as a 1D chain in solution and, as a consequence, (ii) the preservation of the molecular structure and confirmation of the trans-disposition of the 9Accm coordinated ligands.

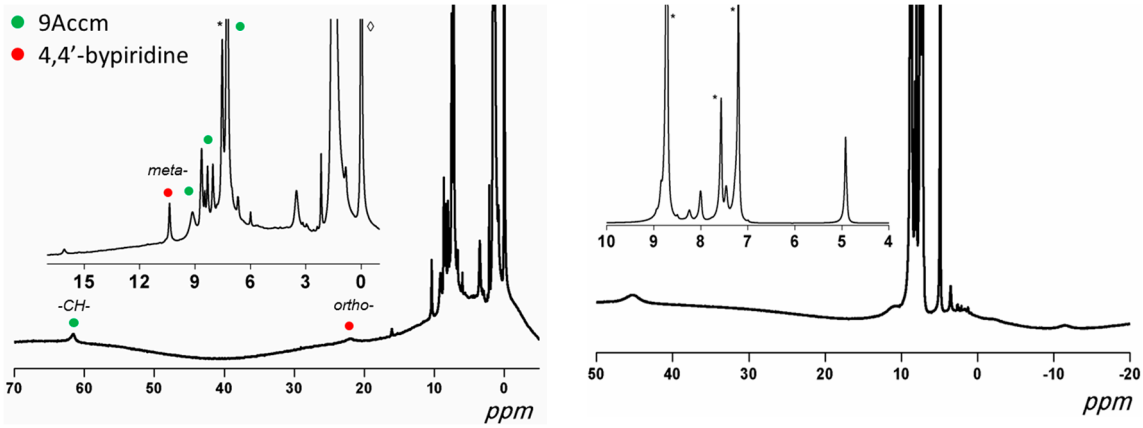

Figure 2. (**A**) Paramagnetic ^{1}H NMR of **1** in $CDCl_3$ between 0 and 70 ppm. (**B**) Paramagnetic ^{1}H NMR of **2** in C_5D_5N between −20 and 50 ppm. * Solvent, ◊ TMS.

Figure S2 shows the spectrum of **2** under the same conditions. To our surprise, the system containing Ni^{II} ions did not display paramagnetic features, having all the signals in a window between 10 and 0 ppm, which is expected for diamagnetic systems. This brought us to question the possible stability of the "$[Ni(9Accm)_2]$" unit solution, where the Ni^{II} ions in this unit could be in a square planar environment displaying a diamagnetic response. To prove our supposition, we designed an additional NMR experiment for compound **2** using C_5D_5N as a solvent for the study of the evolution of the system over time. In the short period of dissolving **2** in C_5D_5N and starting the measurement, the spectrum already showed paramagnetic features (Figure 2B) displaying two broad peaks at 45, 11 and −12 ppm, and a set of sharper signals in the 9–7 ppm range. The shift of such signals was constant over time and after hours. Contrasting this data with the information available, we could preliminarily assign these most shifted peaks at the down field area to the protons of the –CH– of the 9Accm and the *ortho* from the pyridine, respectively. The spectrum did not show additional shifts, indicating that only one species was probably achieved. Further assignments of the structure are complicated at this point, where there are several possible stable units that may be formed with a general $[Ni(9Accm)_2(C_5D_5N)_n(H_2O)_m]$ structure (where n, m = 0, 1 or 2). The *trans* or *cis* disposition of the molecules is also another point that cannot be resolved with the collected data, where related mononuclear Co^{II}-9Accm systems with *cis* conformation of the coordinated CCMoids displayed chemical shifts at high negative fields [22]. Complementary experiments are carried out toward the isolation of a novel monomeric nickel compound for the identification of the final system. The same experiment was carried out with **1**, but in this case the initial signals did not vary after several hours. Therefore, we proved the existence and stability of the diamagnetic $[Ni(9Accm)_2]$ units and show the difference between **1** and **2**, where the first is stable in solution and the second has the tendency of dissociating. Table S3 shows the shift of all the signals.

2.3.2. UV-Vis Absorption Spectra and Fluorescence

The absorption and emission studies in CH_2Cl_2 were made exclusively with compound **1**, taking into account that **2** dissociates in solution and the final species are not properly characterized yet. The electronic absorption spectrum of **1** (10^{-5} M) in distilled CH_2Cl_2 shows an absorption band

at 265 nm (Figure 3A) and two broad and overlapped bands between 300 to 500 nm of similar intensity (Figure 3, inset). From the latest, the highest energy band corresponds to the anthracene groups (300–400 nm) and displays several maxima features of vibronic nature. The second, of lower energy, has a maximum at ~440 nm, which is typical in CCMoid systems and is associated, as are the rest of bands, with π-π* transitions [17,20].

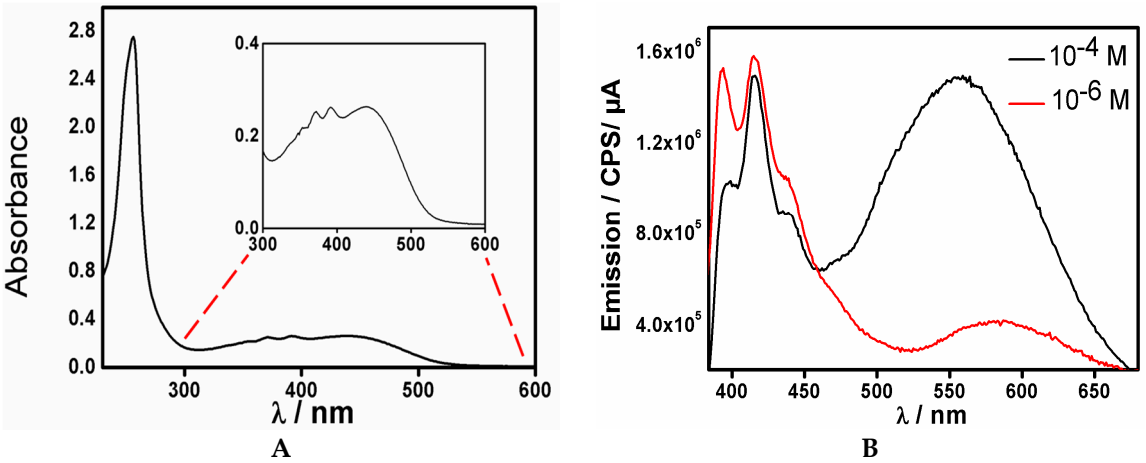

Figure 3. (**A**) Absorption spectrum of **1** in distilled CH_2Cl_2. The inset emphasizes the 300 to 600 nm area. (**B**) Emission spectra of **1** at 10^{-4} M (black) and 10^{-6} M (red) under the same conditions.

Figure 3B shows the fluorescence emission spectra of **1** in distilled CH_2Cl_2 when excited at 350 nm at 10^{-4} (black) and 10^{-6} M (red) concentrations. In the former, it is possible to observed two distinguished emissions of similar intensity. The highest in energy is centered at ~405 nm which splits in a set of three bands with maxima between 390 and 450 nm, correspondingly (10^{-4} M, black line). The lowest emission band appears as a broad signal between 500 to 650 nm, with a maximum at 596 nm. The existence of two luminescent processes at such a wavelength can be related to the emission of the anthracene groups, exhibiting well-resolved vibronic bands and the existence of excimer-/exciplex-like emissions at the lowest energies [27]. Excimers are described as supramolecular dimeric structures where at least one of the molecules is excited, at the applied wavelength, resulting in broad bands shifted from the expected emission toward the red region [28]. On the other hand, an exciplex is a related case/effect but the two molecules are not identical [29]. The formation of excimers in highly conjugated systems, such as anthracene, has been extensively described [30]. The possibility of having intermolecular interactions among the chains and through the anthracene molecules is already observed in the structure where σ-π interactions between anthracene groups are seen (Figure 1B). At the same time, the existence of supramolecular interactions between the anthracene and the 4,4´-bpy groups of different chains is remarkable in **1**. Previously reported investigations on pyrene/4,4´-bpy supramolecular interactions have demonstrated that they can greatly affect the emission properties of the molecules [27]. The discrimination between excimer and exciplex or the exhaustive study of such supramolecular effects on the luminescent properties of compound **1** are not relevant for the present work. On the other hand, emission studies of **1** at different concentrations show the supramolecular nature of the broad band at 596 nm (Figure 3B). Interestingly, the free ligand 9Accm and the monomeric [Co^{II}-9Accm] species published display only one broad band which appears around 600 nm [15,22]. In earlier studies, variations of the concentration in the free ligand, 9Accm, did not provided evidence of an excimer nature [17,19]. The emission at the highest energy band and the evidence of the excimer/exciplex nature of the emission band at the lowest energy will require deeper insight on the fluorescence properties of such systems as well as theoretic calculations to corroborate the studies. Finally, compound **1** shows that the Co^{II} centres act as quenchers, displaying chelation enhancement of quenching (CHEQ) effects, well known with paramagnetic systems.

A comparison of the emission bands of the free 9Accm and **1** shows a clear decrease of the emission (Figure S3).

2.4. Studies in the Solid State

Recently, the magnetic properties of two mononuclear systems with formulae, $[Co(9Accm)_2(py)_2]$ and $[Co(9Accm)_2(2,2'\text{-bpy})]$, have been studied and published by us, showing that both systems behave as SMMs, exhibiting remarkable large and positive zero-field splitting parameters (D = 75 cm^{-1} and 25 cm^{-1}, respectively, Ising plane anisotropy character) [22]. Regarding this, compound **1** relates to those because it contains the same unit, $[Co(9Accm)_2]$, where the 9Accm ligands organize in a *trans* configuration around the Co^{II} ion, similar to the mononuclear compound which displays the largest ZFS value; however, in the case of **1** the Co^{II}-9Accm units are organized in a 1D chain connected between them with a very weak/null magnetic linker (4,4'-bpy) [31,32]. The magnetic studies on **1** were performed with the aim of describing the effects of such a linker on the final anisotropy. On the other hand, compound **2** is isostructural with **1** and was studied for comparative purposes.

2.4.1. Static Magnetic Properties

The dc magnetic susceptibility response of **1** was measured in the temperature range of 1.8–300 K under applied fields of 0.03 (2–30 K) and 0.5 T (2–300 K). At RT, $\chi_M T$ was found to be 2.87 cm^3 mol^{-1} K, which is higher than the value expected for one Co^{II} ion (1.875 cm^3 mol^{-1} K, g = 2.00), which was expected due to the significant spin-orbit contribution usually present in such types of metal centres, similar to the value previously obtained for $[Co(9Accm)_2(py)_2]$ [22,33]. Upon lowering the temperature, $\chi_M T$ smoothly decreases until a value of 2.63 cm^3 mol^{-1} K 100 K. Afterward, the decay of $\chi_M T$ becomes pronounced, being more noticeable from 10 K to 2 K, and reaching a final value of 1.23 cm^3 mol^{-1} K (Figure 4A). Further, $M/N\mu_B$ vs. H data at 2 K presents saturation at the highest magnetic fields with a value close to 2 μ_B, indicating the existence of considerable orbital contributions (Figure 4A, inset). M vs. H/T data was also collected as reduced magnetization with $M/N\mu_B$ vs. H/T in the 0.5–5 T and 1.8–6.8 K ranges toward the study of the axial and rhombic parameters (D and E). The isofield curves did not overlap, indicating the presence of relevant spin-orbital contributions as well (Figure 4A, inset). On the other hand, further representation of $\ln(\chi_M T)$ vs. $1/T$ with different dc fields (0.03, 0.5 and 0.2 T, dc and ac data, respectively) did not provide the features expected for a 1D chain with Ising-like anisotropy (Figure S4).

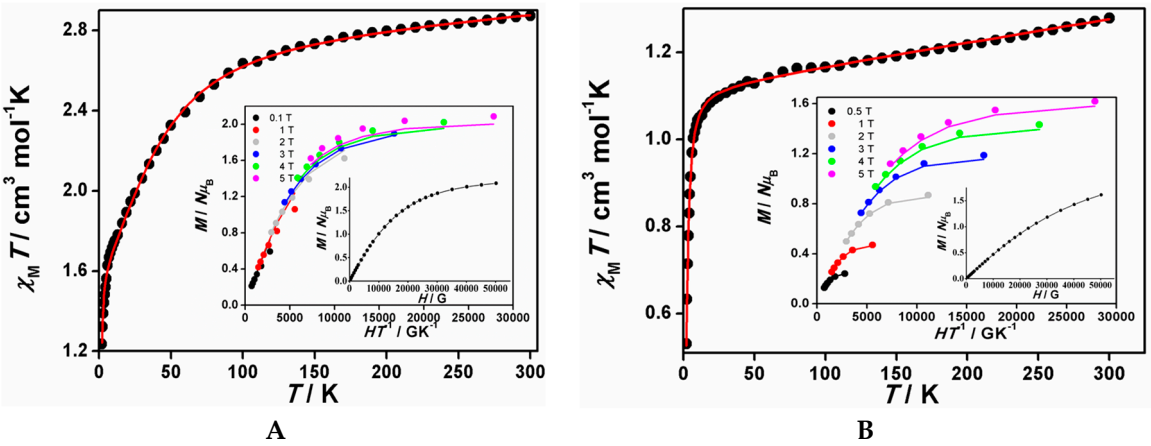

Figure 4. The $\chi_M T$ vs. T graph and insets, $M/N\mu_B$ vs. H/T and $M/N\mu_B$ vs. H data for **1** (**A**) and **2** (**B**). Experimental data are shown as dots and the resulting fitting by a line.

The magnetic data of compound **1** was fitted by the use of the program PHI [34], treating **1** as a mononuclear system even though structurally it is a stable 1D chain in solid state and solution (paramagnetic ^{1}H NMR). We made this decision based on the following facts: (i) the experimental $M/N\mu_B$ vs. H and ln($\chi_M T$) vs. $1/T$ information indicates a considerable spin-orbital contribution, implying an absence of Ising-like anisotropy; (ii) there is consistency of the data compared with previous information about the Ising plane anisotropy values from the mononuclear family of [Co(9Accm)$_2$] mentioned before, and (iii) in each chain, the Co^{II} centres are connected through 4,4'-bpy molecules, known to provide very weak/null antiferromagnetic interactions [31,32]. The crystallographic data reinforces such an idea, showing that the two aromatic rings of 9Accm ligands are twisted >25° (hindering the possibility of small exchange couplings).

In this way, reasonable fitting parameters were extracted by the correlation of the $\chi_M T$ vs. T data and the $M/N\mu_B$ vs. H/T data simultaneously, where g_{av} = 2.42, D = 44.3 cm^{-1}, E = 0.81 cm^{-1} and TIP = 546·10^{-6} cm^3 mol^{-1} (Figure 4A). Poor or unrealistic fittings were found with negative values of the anisotropic parameters. Therefore, system **1**, as the related mononuclear system, presents a large and positive D value [22]. These results also agree with other Co^{II} ions coordinated to β-diketone groups [13]. The intermediate value of the ZFS parameter D in **1** (44 cm^{-1}), compared with its mononuclear predecessors (75 and 25 cm^{-1}), may indicate that even tiny intramolecular effects (from the 4,4'-bpy between the Co^{II} centres) and/or intermolecular interactions among the chains have a great effect on the anisotropy.

The 300 K $\chi_M T$ value of **2** of 1.28 cm^3 mol^{-1} K is larger than the expected only value of 0.99 cm^3 mol^{-1} K for a S = 1, showing the existence of spin-orbit coupling contributions and similar to others reported for Ni^{II} compounds [35,36]. Now, the magnetic susceptibility decreases gradually with temperature until 10 K (1.09 cm^3 mol^{-1} K) and then drops reaching a value of 0.54 cm^3 mol^{-1} K at 2 K. The $M/N\mu_B$ vs. H data at 2 K does not follow Brillouin´s curve, not reaching clear saturation even at the lowest temperature. The experimental reduced magnetization $M/N\mu_B$ vs. H/T using the same range than for **1** shows the existence of appreciable anisotropy with isofield curves not superimposing. The fitting of the data was done in a similar manner as described before. As a result, the best fitting shows g_{av} = 2.12, D = 4.65 cm^{-1}, E = 0.71 cm^{-1}, TIP = 545·10^{-6} cm^3 mol^{-1} and ρ = 1.62% (Figure 4B). Such values and the sign of the ZFS parameter agree well with others for Ni^{II} systems found in the literature [35–38].

Comparison of the results of **1** and **2**, clearly show the anisotropic differences between Co^{II} and Ni^{II} centres, where **2** displays relevant anisotropy, higher than other Ni^{II} systems described in the literature [36] but still significantly lower than **1** [39].

2.4.2. Dynamic magnetic properties

The ac magnetic susceptibility of **1** and **2** below 5 K was investigated in the presence and absence of external dc fields. Compound **1** was the only one showing frequency dependent out-of-phase signals (Figure 5B) under the presence of a dc magnetic field of 0.2 T. In a previous step, experiments to find out the optimal external magnetic field were performed as explained elsewhere (Figure S5) [22]. Ac magnetic susceptibility data was collected by varying frequencies from 10 to 1488 Hz. **1** presents slow relaxation of the magnetization with the characteristic frequency dependence of the in-phase (χ'_M) and out-of-phase (χ''_M) susceptibilities. No maxima were obtained above 2 K, therefore, experiments at lower temperatures and/or extended frequency range have to be performed toward the proper assignment of **1** as a 1D chain SMM system.

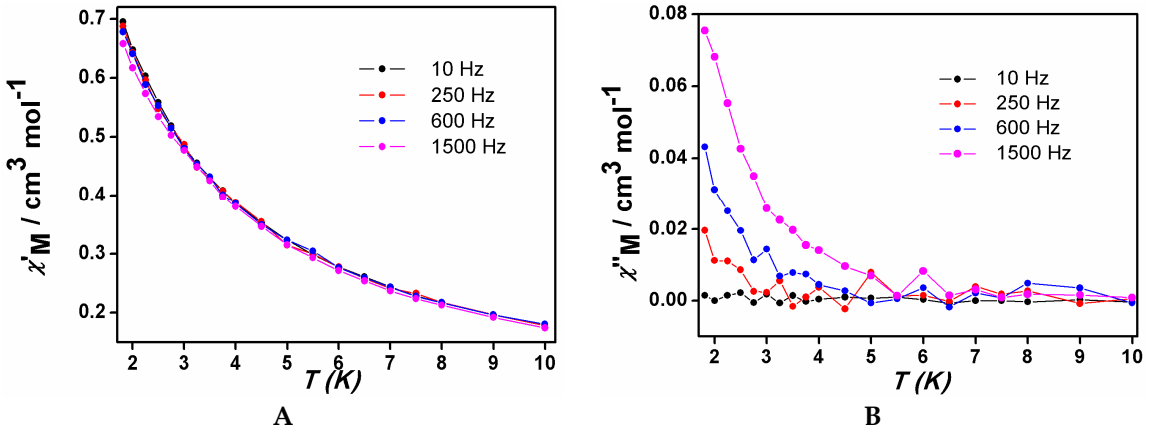

Figure 5. Frequency dependence of the in-phase (**A**) and out-phase (**B**) (χ'_M vs. T and χ''_M vs. T) susceptibilities for **1** under a 0.2 T dc field.

2.5. AFM deposition studies on HOPG

AFM experiments were performed depositing compound **1** on highly oriented pyrolytic graphite (HOPG) wafers. The experiments were performed with the aim of finding structural differences between the 1D system (**1**) and the mononuclear analogue [Co(9Accm)$_2$(py)$_2$] [22]. Spin-coating experiments were performed by depositing **1** dissolved in distilled CH_2Cl_2, where the compound was deposited on freshly cleaved HOPG as described elsewhere [18]. Blank experiments using exclusively the solvent at the same conditions were also performed. The HOPG experiments (Figure 6) display the affinity of **1** for such surface due to the π-π interactions of the anthracene groups with the substrate as described with other *M*-9Accm (*M* = metal) systems in the past [17,18,20,22].

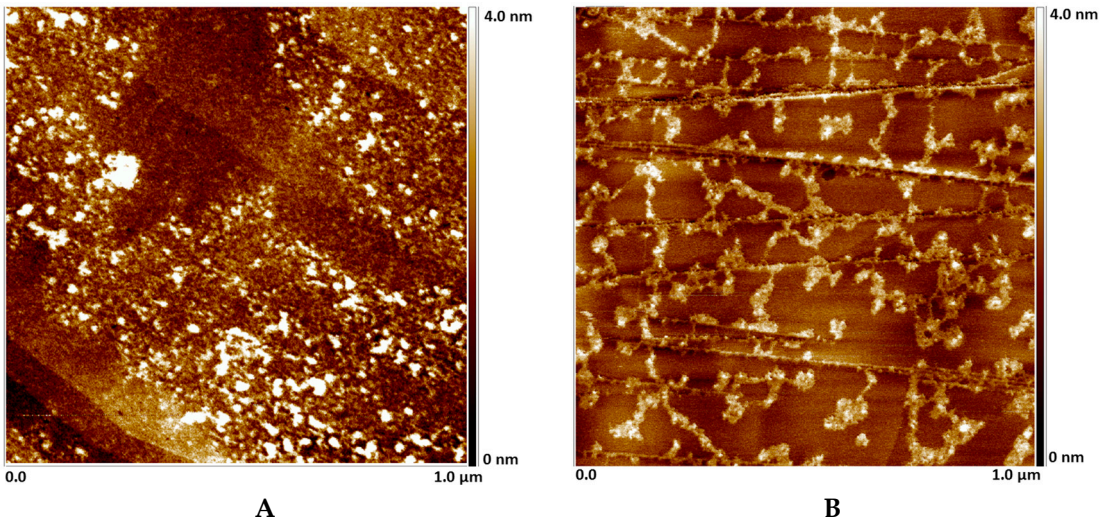

Figure 6. AFM images of HOPG (highly oriented pyrolytic graphite) surfaces after adding (**A**) 10^{-5} M concentration of **1** in CH_2Cl_2 and (**B**) 10^{-6} M of **1** in CH_2Cl_2. Spin coating depositions were performed using different concentrations of **1**. Depositions on freshly cleaved HOPG were performed at 500 rpm during 30 s, where drops of the solutions were added at regular intervals of approximately 10 s.

At 10^{-5} M full cover of the surface was observed and we performed studies of number of layers and heights by changing from tapping to contact mode (Figure 6A and Figure S6) [18,22]. These experiments show that the average height is of ~3.0 nm, implying a number of two to three 1D chains pilled on the substrate. At lower concentrations, 10^{-6} M (Figure 6B and Figure S7) multiple

aggregates of **1** are observed with heights between 1.4 and 2.0 nm, implying one or maximum two pilled chains. The measurement does not allow specifics on the polymeric structure however, overall the shape of the observed arrays differ from previous systems where now, a part from amorphous agglomerations observed in the past [22], there seems to be a preferred length of such clusters (Figure 6B). Also, in the case of previous mononuclear analogous, concentrations to obtain images with aggregates required higher amounts (10^{-4} M) than in the case of **1**.

3. Materials and Methods

C, H and N analyses were performed with a Perkin-Elmer 2400 series II analyser (PerkinElmer, Madrid, Spain). Mass spectra were recorded in $CHCl_3$/MeCN (1:1) using matrix assisted laser desorption ionization with time of flight (MALDI-TOF) mass spectrometer (4800 *Plus* MALDI TOF/TOF (AB Sciex Spain S.L., Madrid, Spain). DHB stands for 2,5-dihydroxybenzoic acid. Infrared spectra (4000–400 cm^{-1}) were recorded from KBr pellets on a Bruker IFS-125 FT-IR spectrophotometer (Bruker Biosciences Espanola S.A, Madrid, Spain). Fluorescence emission spectra were carried out on a Horiba-Jobin-Yvon SPEX Nanolog-TM (Horiba Ltd., MTB Espana, Madrid, Spain). AFM images were captured in tapping mode using a Multimode AFM attached to Nanoscope IV electronics (Digital Instruments, Santa Barbara, CA, USA). Single beam silicon oxide AFM probes were used (T300R-W series, VistaProbes, Phoenix, AZ, USA) with a nominal spring constant of 40 nN/nm. In order to preserve the structure of the sample, the free amplitude of the AFM probe was kept to a minimum and images where acquired at the maximum amplitude set-point. Scan rate was set to 0.7 Hz and resolution was 512 × 512 pixels. Blanks containing the solvent, CH_2Cl_2 (from same butch used for the compounds) following rigorously the exact procedure were performed for each experiment. dc and ac magnetic measurements were performed with Quantum Design MPMS-5S and MPMS-XL magnetometers (LOT-QuantumDesign, Iberia, Madrid, Spain) either at the Universitat Barcelona.

Crystallography. Data for compound **1** were collected at 100 K on Beamline 11.3.1 at the Advanced Light Source, on a Bruker D8 diffractometer (Bruker, Madison, WI, USA) equipped with a PHOTON 100 CCD detector and using silicon 111 monochromated synchrotron radiation (λ = 0.7749 Å). The crystals were mounted on a MiTegen kapton loop (MiTeGen, Ithaca, NY, USA) and placed in the N_2 stream of an Oxford Cryosystems Cryostream Plus (OxfordCyrosystems, Oxford, UK). Data reduction and absorption corrections were performed with SAINT (Bruker ACS Inc., Madison, WI, USA, 2014) and SADABS (Bruker ACS Inc., Madison, WI, USA, 2014), respectively. The structure was solved by intrinsic phasing with SHELXT and refined by full-matrix least-squares on F^2 with SHELXL-2014 [40]. The central carbon atoms of the diketone ligand are disordered over two equivalent positions. The 4,4'-bipyridine also has its two rings disordered over two positions by rotation along its central axis, with relative occupancies 0.77/0.23. Displacement parameters restraints were used to refine these disordered moieties. A number of weak residual electron density peaks (<1.2 e) remained at the end of the refinement in the void space. Attempt at modelling these as DMF lattice solvent were unsuccessful, and the corresponding void space was analysed and taken into account with PLATON/SQUEEZE (Utrecht University, Utrecht, The Netherlands, 2008), that recovered a total of 472 electrons per cell over four voids of 479 cubic angstrom each. These figures, in particular the void volume (2 DMF molecule molecules are unlikely to fit within such a void), would agree with one diffuse DMF molecule per void, thus four per cell. One lattice DMF molecule per formula unit was thus added to the formula. Single crystal diffraction data for compound **2** were collected on a Bruker APEXII SMART diffractometer using a microfocus Molybdenum Kα radiation source. The structures were solved by direct methods (SHELXS97) and refined on F^2 (SHELX-97). Hydrogen atoms were included on calculated positions, riding on their carrier atoms. All details can be found in CCDC 1484521 & 1484522 that contains the supplementary crystallographic data for this paper. These data can be obtained free of charge from The Cambridge Crystallographic Data Centre via https://summary.ccdc.cam.ac.uk/structure-summary-form. Crystallographic and refinement

parameters are summarized in Table S1. Selected bond lengths and angles and intermolecular distances are given in Table S2.

4. Conclusions

Compounds **1** and **2**, with general formula as depicted $[M(9Accm)_2(4,4'\text{-bpy})]_n$ (M = Co^{II} (**1**) and Ni^{II} (**2**)), are the two first examples of 1D systems created by the addition of "$[M(9Accm)_2]$" building blocks connected through a neutral bridging ligand, in this case 4,4'-bpy. They were synthesized by using two different techniques: solvothermal methodology and a microwave assisted method.

The stabilization of the so-called "$[Co(9Accm)_2X_m]$" unit (X = solvent) was proved in the past for some Co^{II} systems containing 9Accm where we observed that it was possible to achieve first the neutral $[Co(9Accm)_2(DMF/H_2O)_m]$ (m = 1 or 2) building block (*trans* conformation by paramagnetic ^{1}H NMR) and later the *cis* version by adding 2,2'-bpy in a second step ($[Co(9Accm)_2(4,4'\text{-bpy})]$). In here, we explored the stability of the Co^{II} and Ni^{II} 1D analogous in solution using this technique as a fingerprint. System **1** displaying signals from 0 to 70 ppm with *trans* features (as it appears in the crystal structure with the assignment accomplished by comparing with previous data) with constant values after several hours. However, when we dissolved **2** in $CDCl_3$ the spectra did not display paramagnetic behaviour and instead showed diamagnetic features. We proposed that units of the type "$[Ni(9Accm)_2]$" (where Ni^{II} has square planar symmetry) resulted from dissociation in solution and proved that we could come back to paramagnetic when C_5D_5N was used (tentative formula: $[Ni(9Accm)_2(C_5D_5N)_n(H_2O)_m]$, with n, m = 0, 1 or 2). Due to the test and results, following experiments in solution were only performed with **1**, which showed that the system displays emission partially quenched by the paramagnetic centres (chelation enhancement of quenching (CHEQ) effects). Also, deposition studies on HOPG of solutions of **1** displayed variations from previous mononuclear analogous, indicating the effect of the chains in the final compound-substrate interactions. Finally, systems **1** and **2** were studies using SQUID and their magnetic characterization provided for both relevant and positive anisotropic values, where **1** presented slow relaxation of the magnetization. From our magnetic characterization we must conclude that system **1** is better described as organized 1D SMM. Toward our initial goals, our next step is the creation of a new generation of 1D coordination chains using metal centres that will provide Ising-axis anisotropy (keeping the $[M(CCMoid)_2]$ unit) and/or the use of linkers that may favour, intramolecular interactions.

Supplementary Materials: The following are available online at www.mdpi.com/2312-7481/2/3/29/s1, Figure S1: Crystal structure of compound **2**, Figure S2: ^{1}H NMR spectrum of **2** in $CDCl_3$, Figure S3: Comparison of the Fluorescence emission of compound **1** and 9Accm in CH_2Cl_2, Figure S4: Representation of $\ln(\chi_M T)$ vs. $1/T$ with different dc fields of compound **1**, Figure S5: Representation χ''_M vs. T at different magnetic fields H_{DC} of compound **1**, Figure S6: (A) AFM experiments (tapping mode) of system **1** at 10^{-5}M. (B) Heights measured: Blue 3.025 nm; Red 3.170 nm and Green 2.152 nm, Figure S7: (A) AFM experiments (tapping mode) of compound **1** at 10^{-6}M. (B) Heights measured: Blue 1.885 nm; Red: 1.437 nm and Green: 1.992 nm, Table S1: Crystal data and structure refinement for compounds **1** and **2**, Table S2: Selected interatomic distances [Å] and angles for compound **1** and compound **2**, Table S3: ^{1}H NMR peaks of compounds **1** and **2**.

Acknowledgments: The authors thank N. Clos from the Serveis Científicotècnics de la UB for her great assistance regarding the magnetic data and are grateful to O. Roubeau (ICMA, CSIC and Universidad de Zaragoza) for his help in the data acquisition and refinement of the structure of compound **1**. This work was supported by the MINECO (Spain) (Projects CTQ2012-32247, and MAT2013-47869-C4-2-P) and from the FONDECYT REGULAR grant 1110206. N.A.-A. acknowledges support of the Spanish MINECO through the Severo Ochoa Centers of Excellence Program under Grant SEV-2015-0496. The Advanced Light Source (S.J.T.) is supported by the Director, Office of Science, Office of Basic Energy Sciences of the U.S. Department of Energy under Contract DE-AC0205CH11231.

Author Contributions: N. Aliaga-Alcalde and M. Soler conceived and designed the experiments; R. Díaz-Torres, M. Menelaou and A. González-Campo performed the experiments; S.J. Teat and E.C. Sañudo analysed the crystallographic data; N. Aliaga-Alcalde and M. Soler wrote the paper.

Conflicts of Interest: The authors declare no conflict of interest.

References

1. Pedersen, K.S.; Bendix, J.; Clérac, R. Single-Molecule magnet engineering: building-block approaches. *Chem. Commun.* **2014**, *50*, 4396–4415.
2. Coulon, C.; Pianet, V.; Urdampilleta, M.; Clérac, R. Single-Chain Magnets and Related Systems. In *Molecular Nanomagnetis and Related Phenomena*; Springer GmbH: Berlin, Germany, 2015; Volume 164, pp. 143–184.
3. Metzger, R.M. Unimolecular Electronics. *Chem. Rev.* **2015**, *115*, 5056–5115. [CrossRef]
4. Schwarz, F.; Lörtscher, E. Break-junctions for investigating transport at the molecular scale. *J. Phys.: Condens. Matter* **2014**, *26*, 474201. [CrossRef]
5. Clemente-Juan, J.M.; Coronado, E.; Gaita-Ariño, A. Magnetic polyoxometalates: From molecular magnetism to molecular spintronics and quantum computing. *Chem. Soc. Rev.* **2012**, *41*, 7464–7478. [CrossRef]
6. Bogani, L.; Wernsdorfer, W. Molecular spintronics using single-molecule magnets. *Nature Mat.* **2008**, *7*, 179–186. [CrossRef]
7. Atanasov, M.; Aravena, D.; Suturina, E.; Bill, E.; Maganas, D.; Neese, F. First principles approach to the electronic structure, magnetic anisotropy and spin relaxation in mononuclear 3d-transition metal single molecule magnets. *Coord. Chem. Rev.* **2015**, *289–290*, 177–214. [CrossRef]
8. Dreiser, J. Molecular lanthanide single-ion magnets: From bulk to submonolayers. *J. Phys.: Condens. Matter* **2015**, *27*, 183203. [CrossRef]
9. Harriman, K.L.; Murugesu, M. An Organolanthanide Building Block Approach to Single-Molecule Magnets. *Acc. Chem. Res.* **2016**. [CrossRef]
10. Gómez-Coca, S.; Cremades, E.; Aliaga-Alcalde, N.; Ruiz, E. Mononuclear Single-Molecule Magnets: Tailoring the Magnetic Anisotropy of First-Row Transition-Metal Complexes. *J. Am. Chem. Soc.* **2013**, *135*, 7010–7018. [CrossRef]
11. Fataftah, M.S.; Zadrozny, J.M.; Rogers, D.M.; Freedman, D.E. A Mononuclear Transition Metal Single-Molecule Magnet in a Nuclear Spin-Free Ligand Environment. *Inorg. Chem.* **2014**, *53*, 10716–10721. [CrossRef]
12. Habib, F.; Korobkov, I.; Murugesu, M. Exposing the intermolecular nature of the second relaxation pathway in a mononuclear cobalt (II) single-molecule magnet with positive anisotropy. *Dalton Trans.* **2015**, *44*, 6368–6373. [CrossRef]
13. Gómez-Coca, S.; Urtizberea, A.; Cremades, E.; Alonso, P.J.; Camon, A.; Ruiz, E.; Luis, F. Origin of slow magnetic relaxation in Kramers ions with non-uniaxial anisotropy. *Nature Commun.* **2014**, *5*, 4300. [CrossRef]
14. Jiang, G.; Song, Y.; Guo, X.; Zhang, D.; Zhu, D. Organic Functional Molecules toward Information Processing and High-Density Information Storage. *Adv. Mat.* **2008**, *20*, 2888–2898. [CrossRef]
15. Aliaga-Alcalde, N.; Marqués-Gallego, P.; Kraaijkamp, M.; Herranz-Lancho, C.; den Dulk, H.; Gorner, H.; Roubeau, O.; Teat, S.J.; Weyhermüller, T.; Reedijk, J. Copper Curcuminoid Containing Anthracene Groups: Fluorescent Molecules with Cytotoxic Activity. *Inorg. Chem.* **2010**, *49*, 9655–9663. [CrossRef]
16. Prins, F.; Barreiro, A.; Ruitenberg, J.W.; Seldenthuis, J.S.; Aliaga-Alcalde, N.; Vandersypen, L.M.K.; van der Zant, H.S.J. Room-Temperature Gating of Molecular Junctions Using Few-Layer Graphene Nanogap Electrodes. *Nano Letters* **2011**, *11*, 4607–4611. [CrossRef]
17. Aliaga-Alcalde, N.; Rodríguez, L.; Ferbinteanu, M.; Hofer, P.; Weyhermüller, T. Crystal Structure, Fluorescence and Nanostructuration Studies of the First Zn^{II} Anthracene-Based Curcuminoid. *Inorg. Chem.* **2012**, *51*, 864–873. [CrossRef]
18. Menelaou, M.; Ouharrou, F.; Rodríguez, L.; Roubeau, O.; Teat, S.J.; Aliaga-Alcalde, N. Dy^{III}- and Yb^{III}-Curcuminoid Compounds: Original Fluorescent Single-Ion Magnet and Magnetic Near-IR Luminescent Species. *Chem. Eur. J.* **2012**, *18*, 11545–11549. [CrossRef]
19. Aliaga-Alcalde, N.; Rodríguez, L. Solvatochromic studies of a novel Cd^{2+}-anthracene-based curcuminoid and related complexes. *Inorg. Chim. Acta* **2012**, *380*, 187–193. [CrossRef]
20. Menelaou, M.; Weyhermüller, T.; Soler, M.; Aliaga-Alcalde, N. Novel paramagnetic-luminescent building blocks containing manganese (II) and anthracene-based curcuminoids. *Polyhedron* **2013**, *52*, 398–405. [CrossRef]
21. Tanh, J.; Harold, B.; Staudt, C.; Janiak, C. Metal-organic frameworks in mixed-matrix membranes for gas separation. *Dalton Trans.* **2012**, *41*, 14003–14027. [CrossRef]

22. Díaz-Torres, R.; Menelaou, M.; Roubeau, O.; Sorrenti, A.; Brandariz-de-Pedro, G.; Sañudo, E.C.; Teat, S.J.; Fraxedas, J.; Ruiz, E.; Aliaga-Alcalde, N. Multiscale study of mononuclear Co^{II} SMMs based on curcuminoid ligands. *Chem. Sci.* **2016**, *7*, 2793–2803. [CrossRef]
23. Gangu, K.K.; Maddila, S.; Mukkamala, S.B.; Jonnalagadda, S.B. A review on contemporary Metal-Organic Framework materials. *Inorg. Chim. Acta* **2016**, *446*, 61–74. [CrossRef]
24. Charde, M.; Shukla, A.; Bukhariya, V.; Mehta, J.; Chakole, R. A Review on: A significance of microwave assist technique in green chemistry. *Int. J. Phytopharm.* **2012**, *2*, 39–50. [CrossRef]
25. Shoichiro, Y. Recent aspects of the stereochemistry of Schiff base-metal complexes. *Coord. Chem. Rev.* **1996**, *1*, 415–437. [CrossRef]
26. Schwarzhans, K.E. NMR spectroscopy of paramagnetic complexes. *Angew. Chem. Int. Ed.* **1970**, *9*, 946–953. [CrossRef]
27. Wagner, B.D.; McManus, G.J.; Moulton, B. Zaworotko, Exciplex fluorescence of $\{[Zn(bipy)_{1.5}(NO_3)_2]\cdot CH_3OH\cdot 0.5pyrene\}_n$: A coordination polymer containing intercalated pyrene molecules (bipy = 4,4'-bipyridine). *Chem. Commun.* **2002**, 2176–2177. [CrossRef]
28. Birks, J.B. Excimers. *Rep. Prog. Phys.* **1975**, *38*, 903–974. [CrossRef]
29. Khokhlova, S.S.; Burshtein, A.I. General theory of Weller Scheme I of exciplex formation. *Chem. Phys. Letters* **2011**, *508*, 324–328. [CrossRef]
30. Eisenthal, K.B. Intermolecular and intramolecular excited state charge transfer. *Laser Chem.* **1983**, *3*, 145–162. [CrossRef]
31. Jensen, P.; Batten, S.R.; Moubaraki, B.; Murray, K.S. Synthesis, crystal structures and magnetic properties of first row transition metal coordination polymers containing dicyanamide and 4,4´-bipyridine. *Dalton Trans.* **2002**, 3712–3722. [CrossRef]
32. Aguilà, D.; Barrios, L.A.; Roubeau, O.; Teat, S.J.; Aromí, G. Molecular assembly of two $[Co(II)_4]$ linear arrays. *Chem. Commun.* **2011**, *47*, 707–709. [CrossRef]
33. Plenk, C.; Krause, J.; Rentschler, E. A Click-Functionalized Single-Molecule Magnet Based on Cobalt(II) and Its Analogous Manganese(II) and Zinc(II) Compounds. *Eur. J. Inorg. Chem.* **2015**, 370–374. [CrossRef]
34. Chilton, N.F.; Anderson, R.P.; Turner, L.D.; Soncini, A.; Murray, K.S. PHI: A powerful new program for the analysis of anisotropic monomeric and exchange-coupled polynuclear d- and f-block complexes. *J. Comput. Chem.* **2013**, *34*, 1164–1175. [CrossRef]
35. Miklovič, J.; Valiqura, D.; Boča, R.; Titiš, J. A mononuclear Ni(II) complex: A field induced single-molecule magneti showing two slow relaxation processes. *Inorg. Chem.* **2015**, *44*, 12484–12487. [CrossRef]
36. Miyasaka, H.; Mizushima, K.; Sugiura, K.; Yamashita, M. A series of Ni(II) pyridyloximato (pao-) compounds $[Ni(pao)_2(L)_2]$ (L = unidentate ligand): As a coordination donor building block in the assembly with Mn(III) salen analogues. *Synth. Metals* **2003**, *137*, 1245–1246. [CrossRef]
37. Miyasaka, H.; Saitoh, A.; Yanagida, S.; Kachi-Terajima, C.; Sugiura, K.-I.; Yamashita, M. Nickel(II) and iron(II) mononuclear complexes with 1-methylimidazole-2-aldoximate: New building units for molecule-assembled magnetic materials. *Inorg. Chim. Acta* **2005**, *358*, 3525–3535. [CrossRef]
38. Paharová, J.; Cernák, J.; Boča, R.; Zák, Z. Preparation, structure and magnetic properties of two tetracyanonickellates: One-dimensional Ni(dien)(mea)$Ni(CN)_4$ and ionic $[Ni(aepn)_2][Ni(CN)_4]\cdot H_2O$. *Inorg. Chim. Acta* **2003**, *346*, 25–31. [CrossRef]
39. Chen, M.; Zhao, H.; Sañudo, E.C.; Liu, C.-S.; Du, M. Two isostructural coordination polymers showing diverse magnetic behaviors: weak coupling (Ni^{II}) and an ordered array of single-shain sagnets (Co^{II}). *Inorg. Chem.* **2016**, *55*, 3715–3717. [CrossRef]
40. Sheldrick, G.M. Crystal structure refinement with SHELXL. *Acta Cryst. A* **2015**, *71*, 3–8. [CrossRef]

© 2016 by the authors; licensee MDPI, Basel, Switzerland. This article is an open access article distributed under the terms and conditions of the Creative Commons Attribution (CC-BY) license (http://creativecommons.org/licenses/by/4.0/).